Experimental investigation of single voxels for laser nanofabrication via two-photon photopolymerization

Hong-Bo Sun,[a] Makoto Maeda, and Kenji Takada
PRESTO, Japan Science and Technology Corporation (JST), and Department of Applied Physics, Osaka University, Suita, Osaka 565-0871, Japan

James W. M. Chon and Min Gu
Center for Micro-Photonics, School of Biophysical Sciences and Electronic Engineering, Swinburne University of Technology, PO Box 218, Hawthorn 3122, Australia

Satoshi Kawata
Department of Applied Physics, Osaka University, Suita, Osaka 565-0871, Japan and The Institute of Physical and Chemical Research (RIKEN), Hirosawa, Wako, Saitama 351-0198, Japan

(Received 21 April 2003; accepted 5 June 2003)

We report critical roles that are played by laser system parameters in two-photon laser nanofabrication, which are not significant in rapid prototyping at larger scale, including: (i) polarization-induced lateral deshaping of volume elements, voxels, the primitive building block of micronanostructures, and (ii) lateral size reduction of voxels at low numerical aperture lens focusing due to thresholding effect. Also interesting is (iii) simultaneous recording of zeroth- and higher-order diffraction patterns, which was not hindered by the two-order light intensity difference by taking the advantage of the large *dynamic exposure time range* of general resins, a concept that is proposed in contrast to *dynamic power range*. © *2003 American Institute of Physics.*
[DOI: 10.1063/1.1598293]

Although it has been recognized as one of the most promising technologies for producing nanodevices due to the intrinsic three-dimensional (3D) processing capability,[1–7] two-photon photopolymerization is still at its infant stage. High-quality laser nanofabrication needs consideration of performance from both materials and laser system aspects, which is the premise to establish it as an advanced nanoprocessing tool. An example along this line is the recent improvement of fabrication accuracy. A near-100-nm lateral spatial resolution has been achieved by using sub-diffraction-limited two-photon photopolymerization,[5–7] which optically utilizes high numerical aperture (NA) lenses for laser beam focusing, and chemically relies on a radical quenching effect.

Synthesis of highly effective two-photon initiators and sensitizers represents an important direction in the present two-photon research.[4,8–10] Good materials alone, however, are not enough to lead to high-level fabrication, for which understanding of the characteristics of focused laser-induced two-photon photopolymerization at the submicron range, and therefore of the possibility and potential of optical writing, is indispensable. Nevertheless, the work has not been done. In this letter, we report how basic parameters, such as laser beam polarization, NA and exposure time affect the shape and size of volume elements (voxels) of photopolymerization. The results presented are essential for properly designing and depicting nanoscale features of 3D microstructures and devices.

The concern about the issue of polarization arises from the observation that rod widths photopolymerized at different scanning directions may differ by up to more than 10% in logpile photonic crystals.[2] Such a significant deviation is not negligible for photonic and optoelectronic devices, which generally need precise matching to structural parameters. For example, a 5% lattice constant shift would completely disable an add–drop wavelength division multiplex filter.[11] Two-photon polymerized structures consist of voxels, the shape and size of which affect the contour of the object to be written, particularly when the feature dimension is small, for example, $<1\ \mu$m.[7] Voxels are generally considered to resemble a spinning ellipsoid with axis lengths $2a=2b<2c$.[12] However, we experimentally found it not true if a linearly polarized laser beam is employed. In order to examine the effect of polarization, an optical system as shown in Fig. 1(a) was utilized. A 780-nm wavelength, 80-fs pulsewidth, 80-MHz repetition rate femtosecond laser was focused to photopolymerizable resin and scanned, as done in our previous work.[5–7,13] Shown in Fig. 1(b) is the lateral scanning electron microscope (SEM) image of a voxel formed using 1.4-NA optics when vertically polarized (along the x direction) output beam was utilized. The complete and isolated voxels in all current research were obtained by using the ascending scan technology we proposed earlier.[13] From the figure, the voxel axis lengths are measured to $2a=325$ nm (x direction) and $2b=295$ nm (y direction), giving rise to a lateral axis ratio $\mu_{\parallel}=a/b=1.1$. Variation of the beam polarization direction relative to the objective led to corresponding orientation rotation of voxels, while their size and shape remain unchanged [Figs. 1(c)–1(e)].

The polarization-dependent voxel shape could be attributed to depolarization effect that was predicted by electromagnetic focusing theory.[14] It is already known that when the beam incident angle α is small, the focal field (E_x, E_y, E_z) is sufficiently described by a cylindrically symmetric

[a]Author to whom correspondence should be addressed; electronic mail: hbsun@ieee.org

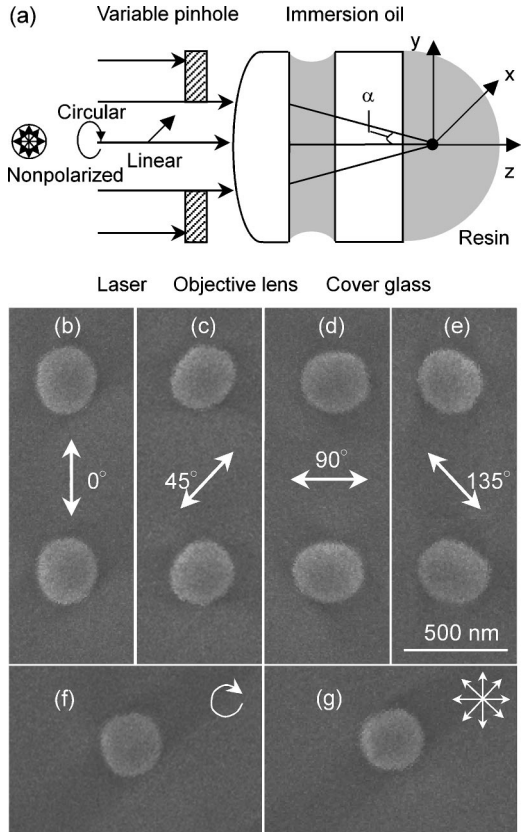

FIG. 1. Polarization-induced lateral deshaping of voxels. (a) Optical setup. Different NAs were realized by adjusting the diameter of the variable pinhole. (b)–(e) Top-view SEM images of voxels formed with laser of different linear polarizations. (f) Voxels produced at incident power the same as (b)–(e), but with a circularly polarized laser and (g) nonpolarized laser. All voxels were created by 1.4-NA focusing 5.0 mW (measured before objective) laser, and the exposure time is 16 ms.

function $[E(r),\ 0,0]$ with $r=\sqrt{(x^2+y^2)}$, where the input beam is assumed to polarize along the x direction. Nevertheless, when $\alpha>40°$ (NA$>$0.7), the symmetry is broken, and a field with significant E_y and E_z component appears. More precisely, the electric field can be expressed as[15]

$$E(r_2,\phi,z_2)=\frac{\pi i}{\lambda}\{[I_0+\cos(2\phi)I_2]\mathbf{i}+\sin(2\phi)I_2\mathbf{j}+2i\cos\phi I_1\mathbf{k}\},\quad(1)$$

where **i**, **j**, and **k** are the unit vectors in the x, y, and z directions, respectively [Fig. 1(a)], variables r_2, z_2, and ϕ are cylindrical coordinates of an observation point. I_0, I_1, and I_2, the average light intensities in ring regions of the zeroth-, first-, and second-order diffractions, respectively, are not constant-zero variables (see definitions in Ref. 15). Hence, it is clear the electric field at the focal region is depolarized. Two-photon point spread function [Fig. 2(a)] calculated according to Eq. (1) shows that the lateral axis ratio is 1.30 at 1.4 NA and 1.06 at 0.8 NA if the FWHM full width at half-maximum (FWHM) was adopted as polymerization threshold line. These values agree with the experimentally attained deshaping degree, 1.1 at 1.4 NA and not discernible when NA$<$1.0.

If the assignment of lateral voxel deshaping to depolarization effect is sound, the nonunit lateral axis ratio could be eliminated by adopting a circular and nonpolarized beam,

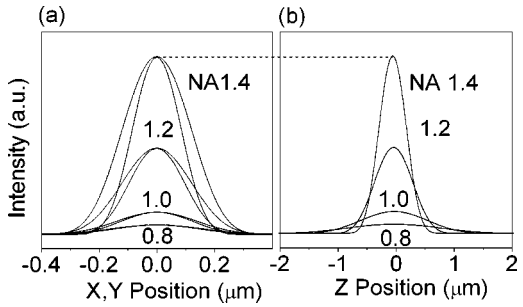

FIG. 2. Theoretical two-photon point spread function calculated using vectorial Debye method. (a) x axis (wider profiles) and y axis (narrower profiles), and (b) vertical direction (z axis). It was assumed that the incident power before the aperture was identical and the laser was focused 10 μm above the glass substrate. The refractive indexes of the resin and the cover glass are 1.512 and 1.49, respectively. The spherical aberration due to the refractive index mismatch is considered, which, however induces, in the case of NA$=$1.2, only a 0.5-μm vertical shift of the focal spot when the focusing depth increases from zero (at the glass/resin interface) until 20 μm deep inside the resin. The focal spot shape and size remain unchanged.

which was experimentally realized by inserting a 780-nm antireflection-coated c-axis-cut quartz $\lambda/4$ retardation plate and a visible-range double-plate-type quartz depolarizer into the light path, respectively. As a result, voxels of nearly perfect round lateral cross section were achieved in both cases [Figs. 1(f) and 1(g)].

In these experiments, the different NAs were realized by a variable pinhole. NA change redistributes the photon energy at the focal volume. Deducing from the FWHM values presented in Fig. 2, a low NA tends to give larger feature sizes in both lateral and vertical directions regardless the absolute intensity level. Experimentally, however, a contradictory result was obtained. At the identical exposure condition (particularly the focal spot powers are kept identical), a low NA (0.88) gives a lateral voxel size of 350 nm, smaller than that achieved at high NA (1.4), 460 nm [Fig. 3(a)], although the smallest visible voxels are 260 nm at 0.88 NA and 120 nm at 1.4 NA, respectively. Further experiment

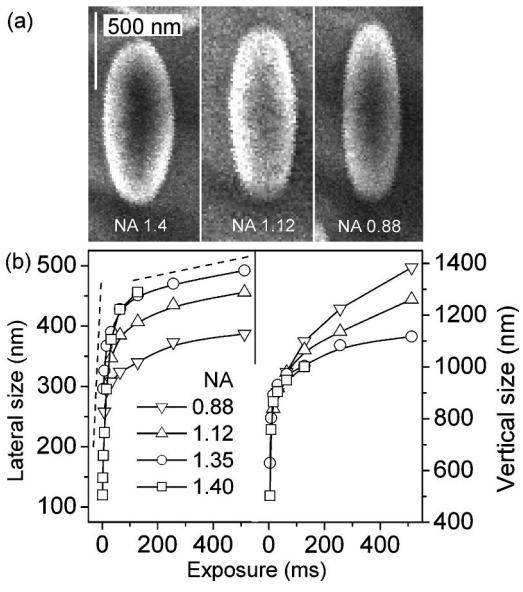

FIG. 3. NA-dependent voxels. (a) Side-view SEM images of voxels formed with identical focal spot laser power. (b) Exposure time-dependent voxel size in both lateral and longitudinal directions under different NAs.

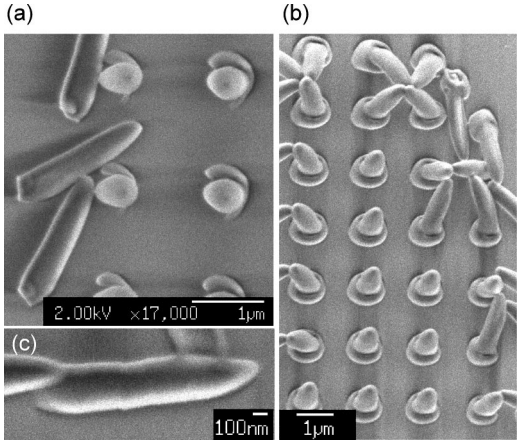

FIG. 4. Simultaneous recording of zeroth- and first-order diffracted fringes at the focal spot. (a) 128-ms and (b) 256-ms exposure, and (c) zeroth-order body of a voxel obtained at 256-ms exposure, where the first order fringe was detached during developing.

shows that it is common that at intermediate irradiation level, low NA provides better lateral resolution [Fig. 3(b)]. This phenomenon could be interpreted by a threshold effect.[5,6] In the case of low NA focusing, laser power is distributed to a larger volume with a solidified front demarcated by the threshold camber vertically expanded and laterally shrunken, as proved by the point spread functions in Fig. 2. This led to slim voxels. This effect provides an example that material attributes affect the nanofabrication performance, and it could find technical use, for example, for separately controlling the lateral and vertical dimensions of single-scan-produced rods in logpile photonic crystals[2] by NA tuning or for producing high-aspect-ratio two-dimensional structures with low-NA focusing.

Increase of voxel size is limited by the power window defined by two-photon polymerization and laser-induced breakdown thresholds. Their ratio is defined as the dynamic power range P_{DPR}, meaning the maximum relative power that can be utilized for microfabrication. Small dynamic power range is usually not a problem for pinpoint writing of nanostructures. However, for multibeam interferential patterning of 3D periodic structures,[16] higher-order diffracted patterns are sometimes helpful to achieve sub-structure-contained photonic lattices.[17] Nevertheless, the nearly two-order light intensity difference makes it impossible to simultaneously polymerize the zeroth- and first-order maxima in a resin that possesses P_{DPR} of only $2\sim5$, typical values for commercial resins. The issue is solved if a concept, dynamic exposure time range (T_{DTR}) is considered. Similar to dynamic power range, the *dynamic time range* can be defined as the exposure temporal span determined by the exposure times that are necessary to induce polymerization and to cause material breakdown, respectively, at a given laser power.

The dynamic time range is also a material-dependent property and is a function of exerted exposure power. T_{DTR} could be larger than P_{DPR} by orders of magnitude; for example, ~1000 times at 1.1 P_{th} for the current material system. At the long exposure duration, the polymerization rate changes pronouncedly versus time increase, for example, 7.5 and 0.09 nm/s at lateral dimension when exposure proceeds to 4 and 256 ms, respectively (the dashed lines in Fig. 3). It predicts that after the size expansion at the central portion of the zeroth-order diffraction reaches a near-saturation status, patterns at sub-maxima starts growth with a higher rate upon exhaustion of radical quenchers. In other words, the long dynamic time range permits simultaneous, or more precisely, sequentially recording in one exposure event both zeroth- and higher-order diffracted features.

Our analysis was experimentally confirmed. Figure 4 shows the SEM images of voxels formed at a relatively longer exposure time, where partly [Fig. 4(a)] and fully [Fig. 4(b)] recorded first-order diffraction fringes are clearly seen. The two-photon polymerization time threshold at $P=10$ mW is around 1 ms. Voxels in Figs. 4(a) and 4(b) are from 128-ms and 256-ms exposures, respectively. Since focal spot height varies point by point, the characteristic of the ascending scan technology, voxels appear either truncated or overturned. Moreover, it was found the zeroth- and first-order features appear exactly at positions expected by calculation,[6] and are well separated, so that a focal spot that is fully lifted from substrate results in a voxel not accompanied by the first-order fringe [Fig. 4(c)]. These findings discriminate the roles that are played by exposure time and laser power in two-photon photopolymerization nanowriting. The large dynamic time range could lead to increased freedom for tailoring complicated patterns, for example, in rapid fabrication of photonic crystals by multibeam interference.

In summary, seemingly simple laser system parameters were found playing previously unrevealed roles for nanoscale writing of voxels. Although our analyses are based on two-photon photopolymerization, they are applicable to the general process of precision laser microfabrication including those launched by single-photon absorption.

[1] S. Maruo, O. Nakamura, and S. Kawata, Opt. Lett. **22**, 132 (1997).
[2] H.-B. Sun, S. Matsuo, and H. Misawa, Appl. Phys. Lett. **74**, 786 (1999).
[3] H.-B. Sun, Y. Xu, S. Juodkazis, K. Sun, M. Watanabe, J. Nishii, S. Matsuo, and H. Misawa, Opt. Lett. **26**, 325 (2001).
[4] B. H. Cumpston, S. P. Ananthavel, S. Barlow, D. L. Dyer, J. E. Ehrlich, L. L. Erskine, Ahmed A. Heikal, S. M. Kuebuler, I.-Y. S. Lee, D. M.-Maugon, J. Qin, H. Rokel, M. Rumi, X. Wu, S. R. Marder, and J. W. Perry, Nature (London) **398**, 51 (1999).
[5] S. Kawata, H.-B. Sun, T. Tanaka, and K. Takada, Nature (London) **412**, 667 (2001).
[6] T. Tanaka, H.-B. Sun, and S. Kawata, Appl. Phys. Lett. **80**, 312 (2002).
[7] H.-B. Sun, K. Takada, and S. Kawata, Appl. Phys. Lett. **79**, 3173 (2001).
[8] K. D. Belfield, K. J. Schafer, Y. U. Liu, J. Liu, X. B. Ren, and E. W. Van Stryland, J. Phys. Org. Chem. **13**, 837 (2000).
[9] O. K. Kim, K. S. Lee, H. Y. Woo, K. S. Kim, G. S. He, J. Swiatkiewicz, and P. N. Prasad, Chem. Mater. **12**, 284 (2000).
[10] W. H. Zhou, S. M. Kuebler, K. L. Braun, T. Y. Yu, J. K. Cammack, C. K. Ober, J. W. Perry, and S. R. Marder, Science **296**, 1106 (2002).
[11] S. Noda, A. Chutinan, and M. Imada, Nature (London) **407**, 608 (2000).
[12] M. Born and E. Wolf, *Principles of Optics*, 7th ed. (Cambridge University Press, Cambridge, 1999.)
[13] H.-B. Sun, T. Tanaka, and S. Kawata, Appl. Phys. Lett. **80**, 3673 (2002).
[14] J. Stamners, *Waves in Focal Region* (Adam Hilger, Bristol, 1986).
[15] M. Gu, *Advanced Optical Imaging Theory* (Springer, Heidelberg, 1999).
[16] S. Shoji and S. Kawata, Appl. Phys. Lett. **76**, 2668 (2000).
[17] H.-B. Sun, A. Nakamura, S. Shoji, X.-M. Duan, and S. Kawata (unpublished).